Granular Matter (2009) 11:157–168
DOI 10.1007/s10035-009-0132-8

The second and third Sonine coefficients of a freely cooling granular gas revisited

Andrés Santos · José María Montanero

Received: 15 December 2008 / Published online: 24 March 2009

Abstract In its simplest statistical-mechanical description, a granular fluid can be modeled as composed of smooth inelastic hard spheres (with a constant coefficient of normal restitution α) whose velocity distribution function obeys the Enskog–Boltzmann equation. The basic state of a granular fluid is the homogeneous cooling state, characterized by a homogeneous, isotropic, and stationary distribution of scaled velocities, $F(\mathbf{c})$. The behavior of $F(\mathbf{c})$ in the domain of thermal velocities ($c \sim 1$) can be characterized by the two first non-trivial coefficients (a_2 and a_3) of an expansion in Sonine polynomials. The main goals of this paper are to review some of the previous efforts made to estimate (and measure in computer simulations) the α-dependence of a_2 and a_3, to report new computer simulations results of a_2 and a_3 for two-dimensional systems, and to investigate the possibility of proposing theoretical estimates of a_2 and a_3 with an optimal compromise between simplicity and accuracy.

Keywords Homogeneous cooling state · Sonine coefficients · Linear approximations

1 Introduction

The prototype model for a granular gas is a system of smooth inelastic hard spheres characterized by a coefficient of normal restitution $0 < \alpha \leq 1$ [1–3]. Kinetic theory arguments similar to those followed in the elastic case allow one to derive the Boltzmann and Enskog equations [4] for the velocity distribution function $f(\mathbf{r}, \mathbf{v}, t)$.

Perhaps the basic and simplest physical state for a granular gas is the homogeneous cooling state (HCS), where the gas is isolated and has an isotropic and spatially uniform distribution [3]. In this state, the collisional loss of energy, characterized by the cooling rate ζ, makes the mean kinetic energy (directly related to the so-called granular temperature T) decay monotonically in time following Haff's law [5]:

$$T(t) = \frac{T(0)}{\left[1 + \frac{1}{2}\zeta(0)t\right]^2}. \tag{1}$$

Therefore, the distribution function evolves in time toward a delta function, i.e., $f(\mathbf{v}) \to n\delta(\mathbf{v})$, where n is the number density. However, the simplicity of this trivial asymptotic state is deceiving since the distribution function actually reaches an interesting scaling (or self-similar) form

$$f(\mathbf{v}, t) = n v_0^{-d}(t) F(\mathbf{c}(t)), \quad \mathbf{c}(t) = \mathbf{v}/v_0(t). \tag{2}$$

Here, d is the dimensionality and $v_0(t)$ is the thermal speed defined by

$$\frac{d}{2} v_0^2(t) = \frac{1}{n} \int d\mathbf{v}\, v^2 f(\mathbf{v}, t). \tag{3}$$

By definition,

$$\langle c^2 \rangle = \frac{d}{2}, \tag{4}$$

where the (scaled) velocity moments are

$$\langle c^{2p} \rangle = \int d\mathbf{c}\, c^{2p} F(\mathbf{c}). \tag{5}$$

In the HCS, the Enskog–Boltzmann equation for the probability distribution function $F(\mathbf{c})$ of the reduced velocity is [6]

A. Santos (✉)
Departamento de Física, Universidad de Extremadura,
06071 Badajoz, Spain
e-mail: andres@unex.es

J. M. Montanero
Departamento de Ingeniería Mecánica, Energética y de los Materiales,
Universidad de Extremadura, 06071 Badajoz, Spain
e-mail: jmm@unex.es

$$\frac{\mu_2}{d}\frac{\partial}{\partial \mathbf{c}}\cdot \mathbf{c}F(\mathbf{c}) = I[\mathbf{c}|F,F], \tag{6}$$

where the collision operator is

$$I[\mathbf{c}_1|F,F] = \int d\mathbf{c}_2 \int d\widehat{\boldsymbol{\sigma}}\,\Theta(\mathbf{c}_{12}\cdot\widehat{\boldsymbol{\sigma}})(\mathbf{c}_{12}\cdot\widehat{\boldsymbol{\sigma}}) \times\left[\alpha^{-2}F(\mathbf{c}_1'')F(\mathbf{c}_2'') - F(\mathbf{c}_1)F(\mathbf{c}_2)\right] \tag{7}$$

and we have introduced the collisional moments

$$\mu_{2p} \equiv -\int d\mathbf{c}\, c^{2p} I[\mathbf{c}|F,F], \tag{8}$$

so that $2\mu_2/d$ is the dimensionless cooling rate. In Eq. 7, $\mathbf{c}_{12}\equiv \mathbf{c}_1-\mathbf{c}_2$ is the relative velocity of the colliding particles, $\widehat{\boldsymbol{\sigma}}$ is a unit vector directed along the line of centers from the sphere 1 to the sphere 2, Θ is the Heaviside step function, and $(\mathbf{c}_1'', \mathbf{c}_2'')$ are the precollisional or restituting velocities yielding $(\mathbf{c}_1, \mathbf{c}_2)$ as the postcollisional ones, i.e.

$$\mathbf{c}_{1,2}'' = \mathbf{c}_{1,2} \mp \frac{1}{2}(1+\alpha^{-1})(\mathbf{c}_{12}\cdot\widehat{\boldsymbol{\sigma}})\widehat{\boldsymbol{\sigma}}. \tag{9}$$

The exact solution of Eq. 6 is not known. Except in the elastic case ($\alpha = 1$), the Maxwellian $F(\mathbf{c}) = \pi^{-d/2}e^{-c^2} \equiv \phi(\mathbf{c})$ is not a solution. In particular, if $\alpha < 1$, it is known that $F(\mathbf{c})$ develops an exponential high-energy tail [6,7],

$$F(\mathbf{c}) \sim e^{-\xi c}, \quad \xi = \frac{d\pi^{(d-1)/2}}{\Gamma(\frac{d+1}{2})\mu_2}. \tag{10}$$

A convenient way of characterizing the deviation of $F(\mathbf{c})$ from $\phi(\mathbf{c})$ in the regime of low and intermediate speeds is through the Sonine polynomial expansion

$$F(\mathbf{c}) = \phi(\mathbf{c})\left[1+\sum_{k=2}^{\infty} a_k L_k^{(\frac{d-2}{2})}(c^2)\right], \tag{11}$$

where $L_k^{(a)}$ are generalized Laguerre (or Sonine) polynomials [8]. The first two non-trivial coefficients are a_2 and a_3. They are related to the fourth and sixth velocity moments as

$$\langle c^4\rangle = \frac{d(d+2)}{4}(1+a_2), \tag{12}$$

$$\langle c^6\rangle = \frac{d(d+2)(d+4)}{8}(1+3a_2-a_3). \tag{13}$$

The Sonine expansion (11) is known to be only asymptotic [9], so that its practical applicability is restricted to low and intermediate velocities (say $c \lesssim 1$), in which case the most relevant coefficients are a_2 and a_3. Therefore, the determination of these two coefficients is important to quantify the basic deviations of the HCS distribution $F(\mathbf{c})$ from the Maxwellian $\phi(\mathbf{c})$, at least for $c \lesssim 1$. This explains the interest this problem has attracted over the years [3,6,9–21]. Apart from this formal motivation, the knowledge of $a_2(\alpha)$ and $a_3(\alpha)$, especially in the case of the former, is needed to evaluate the dependence of the transport coefficients on inelasticity [9,22,23].

The aim of this paper is three-fold. First, some of the efforts done in the last dozen years or so to estimate a_2 and a_3 by theoretical tools and to measure them in simulations are briefly reviewed in Sect. 2. Next, we explore the possibility of deriving theoretical expressions for a_2 and a_3 with an optimal compromise between simplicity and accuracy. To that end, we restrict ourselves to the class of linear approximations, revisit some of the ones already proposed in the literature, and construct a few new ones in Sect. 3. Those approximations are compared with new ($d = 2$) and recently published [18,19] ($d = 3$) computer simulations in Sect. 4. Section 5 addresses the case of granular gases heated with a white-noise thermostat. Finally, the conclusions are summarized in Sect. 6, while some complementary material is relegated to the Appendices.

2 A brief review of previous results

Taking (even) moments in both sides of Eq. 6 one gets the *exact* set of moment equations

$$\mu_{2p} = p\mu_2\frac{\langle c^{2p}\rangle}{\langle c^2\rangle}, \quad p \geq 2, \tag{14}$$

where use has been made of Eq. 4. The condition $p \geq 2$ is introduced because Eq. 14 becomes an identity for $p = 0$ and also for $p = 1$.

It is important to notice that the collisional moments are functionals of the distribution function, so that Eq. 14 implies a coupling among *all* the Sonine coefficients a_k and there is no a priori reason to expect a chosen truncation to provide accurate results for a subset of coefficients. On the other hand, most of the routes followed to get theoretically based results assume some kind of truncation and/or order-of-magnitude simplification. More specifically, one usually *approximates* the first few collisional moments μ_{2p} by inserting the expansion (11) into Eqs. 7 and 8, truncating the expansion after a certain order and, in some cases, neglecting nonlinear terms. The resulting set of approximate equations is then solved algebraically to obtain estimates for the desired coefficients a_k. In principle, these estimates are uncontrolled and can be assessed only after comparison with computer simulations.

The first application of this method was carried out by Goldshtein and Shapiro in a pioneering and extensive paper [10]. They derived a simple expression for a_2 in the three-dimensional ($d = 3$) case by taking a *linear* approximation (namely, neglecting a_2^2 and a_k with $k \geq 3$) in Eq. 14 with $p = 2$. Here we quote their result:

$$a_2 = \frac{16(1-\alpha)(1-2\alpha^2)}{\lambda_0+\lambda_1\alpha+\lambda_2\alpha^2(1-\alpha)}, \tag{15}$$

where $(\lambda_0, \lambda_1, \lambda_2) = (401, -337, 190)$. They noted that, according to their estimate, the magnitude of a_2 was quite small ($|a_2| < 0.04$). However, there was a small algebraic mistake in their derivation that was subsequently corrected by van Noije and Ernst [6], who also generalized the result to arbitrary d. The expression derived by van Noije and Ernst (vNE) maintains the form (15), except that $(\lambda_0, \lambda_1, \lambda_2) = (9 + 24d, 8d - 41, 30)$, what in the three-dimensional case becomes $(\lambda_0, \lambda_1, \lambda_2) = (81, -17, 30)$. This yields values of $|a_2|$ up to five times larger than those predicted by the (wrong) original expression by Goldshtein and Shapiro. Although published in 1998, vNE's result had been circulating earlier and so in 1996 Brey et al. [11] confirmed its accuracy for $d = 3$ and $\alpha \geq 0.7$ by comparison with DSMC simulations [24,25] of the Boltzmann equation. Brey et al. [11] also presented simulation data for $\langle c^6 \rangle$ but they did not extract from them the corresponding values of a_3. When this is done from Figs. 5 and 6 of Ref. [11], one gets $a_3 \simeq -0.005$ for $0.7 \leq \alpha \leq 0.9$ and $d = 3$. More recently, Ahmad and Puri [20,21] carried out large-scale event-driven molecular dynamics simulations and measured a_2 and a_3 in the HCS for $\alpha \geq 0.7$ in two- and three-dimensional systems. The results confirmed the accuracy of vNE's expression of a_2 in that range of inelasticity and showed that a_3 was typically four to five times smaller than a_2. These authors also studied the time evolution of a_k for $k = 2$–5 to monitor the transition from the HCS to an inhomogeneous state.

In 1999, Garzó and Dufty [12] studied the HCS for three-dimensional binary mixtures. Neglecting again a_2^2 and a_k with $k \geq 3$, they obtained explicit expressions for the Sonine coefficient a_2 of both species as functions of the three coefficients of restitution and of the temperature ratio T_1/T_2. To close the problem, it is necessary to determine T_1/T_2 from the condition of equal cooling rates for both species, yielding a highly nonlinear equation. The results showed that typically the component made of particles with a larger mass has a higher temperature and a higher value of a_2. The theoretical predictions were later validated by DSMC simulations [16].

The authors pointed out in 2000 [13] that the linear approximation to get a_2 is not univocally defined, the result depending on the way that the quantities in Eq. 14 are arranged. In particular, if Eq. 14 for $p = 2$ is rewritten as $\mu_4/\langle c^4 \rangle = 2\mu_2/\langle c^2 \rangle$ and then a linear approximation is applied the result is given again by Eq. 15 but with $(\lambda_0, \lambda_1, \lambda_2) = (25 + 24d, 8d - 57, -2)$, implying $(\lambda_0, \lambda_1, \lambda_2) = (97, -33, -2)$ for $d = 3$. This alternative expression is hardly distinguishable from vNE's if $\alpha \gtrsim 0.5$ but provides up to 16% smaller values than the latter for higher inelasticities. We performed DSMC simulations of a_2 for $d = 3$ and $\alpha \geq 0.2$ which exhibited an excellent agreement with our alternative linear approximation. Moreover, DSMC data of a_3 were also presented in Ref. [13]. While $a_3 \simeq -0.005$ for $0.6 < \alpha < 0.9$, a relatively rapid decay of a_3 for higher inelasticities was observed.

Brilliantov and Pöschel [14] were possibly the first ones to depart from the linear approximation. They neglected a_k with $k \geq 3$ but retained a_2^2 in Eq. 14 with $p = 2$, thus obtaining a closed cubic equation for a_2 (and $d = 3$). Its physical root is very close to vNE's expression for $\alpha \gtrsim 0.4$ but becomes up to 10% larger than it for smaller values of α. Taking into account the simulation results presented in Ref. [13], it turns out that the physical root of the cubic equation deviates in the wrong direction from vNE's simpler linear approximation. This paradoxical outcome shows that the Sonine coefficients a_k with $k \geq 3$ are not negligible for $\alpha \lesssim 0.4$.

A different truncation scheme was followed by Huthmann et al. [15], who assumed that $a_k = \mathscr{O}(\varepsilon^k)$, where $\varepsilon \sim |a_2|^{1/2}$ was treated as a small parameter. The solution to order $k \geq 2$ was obtained by taking Eq. 14 for $p = 2, \ldots, k$ and formally neglecting terms of order ε^ℓ with $\ell > k$. The second-order solution recovers the vNE result for a_2. In the third-order solution one has a set of two linear equations for a_2 and a_3, but the fourth-order approximation involves a set of three equations for a_2, a_3, and a_4 that include a_2^2, so that the problem becomes nonlinear for $k \geq 4$. In this approach, the coefficient a_2 is renormalized as the truncation order increases. Huthmann et al. applied their scheme to $d = 2$ and observed that the values of a_2 obtained from order ε^2 to order ε^6 were practically the same as long as $\alpha \gtrsim 0.6$. However, those values were dramatically sensitive to the truncation order for higher inelasticities, thus indicating that the assumption $a_k = \mathscr{O}(\varepsilon^k)$ fails if $\alpha \lesssim 0.6$. Molecular dynamics simulations showed a good performance of vNE's expression for hard disks and $\alpha \geq 0.4$.

Coppex et al. [17] tried an approach to estimate a_2 different from those based on Eq. 14. They started from Eq. 6 in the limit $\mathbf{c} \to \mathbf{0}$ and then inserted the Sonine expansion (11) by neglecting a_2^2 and a_k with $k \geq 3$. The solution of the resulting linear equation for a_2 had the structure of a polynomial of fourth degree in α^2 divided by a polynomial of eighth degree in α (with no α^5 and α^7 terms). Although promising, this alternative method yields poor results for small and moderate inelasticities and only improves over the vNE benchmark formula if $\alpha \lesssim 0.4$, as comparison with DSMC data for $d = 2$ shows [17]. Coppex et al. also elaborated further on the ambiguity of the linear approximation for a_2 pointed out in Ref. [13]. In particular, they showed that the linear approximation as applied to $\mu_4/\langle c^4 \rangle = 2\mu_2/\langle c^2 \rangle$ and to $\mu_4 \langle c^2 \rangle / 2\mu_2 \langle c^4 \rangle = 1$ presented a very good agreement with their two-dimensional simulations.

More recently, Brilliantov and Pöschel [18,19] have considered the linear approximation of Eq. 14 with $p = 2$ and $p = 3$ by neglecting a_2^2, $a_2 a_3$, a_3^2, and a_k with $k \geq 4$. This gives a set of two linear equations for a_2 and a_3 that is actually equivalent to Huthmann et al.'s method to order ε^3. By

comparing with their own DSMC simulations for $d = 3$, Brilliantov and Pöschel showed that their expression of a_2, while rather more complicated than vNE's, provided worse estimates than the latter for $\alpha \lesssim 0.6$. As for their expression of a_3, it was quite good for $\alpha \gtrsim 0.6$ and exhibited the right qualitative behavior for larger inelasticities. Apart from a_2 and a_3, they also measured a_4, a_5, and a_6 in the simulations, showing that their values were not negligible if $\alpha \lesssim 0.6$. In fact, these authors argued that the Sonine expansion breaks down for large inelasticity.

Using the asymptotic high-velocity tail (10), Noskowicz et al. [9] have shown that $a_k \propto (-4/\xi^2)^k (k+1)!$ for large k, so that the series (11) is divergent, although it is asymptotic and Borel resummable. On the other hand, the Sonine expansion of the modified function $G_\gamma(\mathbf{c}) = e^{-(1-\gamma)c^2} F(\mathbf{c})$ does converge for $0 < \gamma < \frac{1}{2}$. Truncating the Sonine expansion of $G_\gamma(\mathbf{c})$ after $k = N_s$ (with $N_s = 10$, 20, and 40), Noskowicz et al. obtained numerically the associated Sonine coefficients $a_k^{(\gamma)}$, $k = 0, 1, \ldots N_s$, with the help of symbolic software. Once $G_\gamma(\mathbf{c})$ is (approximately) determined in this way, the Sonine coefficients a_k of the true distribution function $F(\mathbf{c}) = e^{(1-\gamma)c^2} G_\gamma(\mathbf{c})$ can be obtained by quadratures. The numerical results for a_2, which are well fitted in the three-dimensional case by Eq. 15 with $(\lambda_0, \lambda_1, \lambda_2) = (104.1, -51.43, 78.67)$, confirmed that vNE's expression overestimates a_2 for $\alpha \lesssim 0.5$, while the alternative expression proposed in Ref. [13] is rather accurate (although it slightly overestimates a_2).

3 Theoretical estimates from linear approximations

Our main goal now is to get *estimates* of the Sonine coefficients a_2 and a_3 by the application of approximations that neglect the coefficients a_k with $k \geq 4$ as well as the nonlinear terms a_2^2, $a_2 a_3$, and a_3^2. As we will see, this recipe is not a systematic method and so it does not provide a unique result.

Given a functional $X[F]$ of the scaled probability distribution function $F(\mathbf{c})$, henceforth we will use the notation $\mathscr{L}_{a_2,a_3}\{X\}$ to denote an approximation to $X[F]$ obtained by using Eq. 11 and neglecting a_k with $k \geq 4$ and nonlinear terms (like a_2^2, $a_2 a_3$, and a_3^2). Furthermore, if a_3 is also neglected, the corresponding approximation will be denoted by $\mathscr{L}_{a_2}\{X\}$. In particular, in the case of the collisional moments defined by Eq. 8 with $p = 1$, 2, and 3, one gets

$$\mathscr{L}_{a_2,a_3}\{\mu_2\} = A_0 + A_2 a_2 + A_3 a_3, \tag{16}$$

$$\mathscr{L}_{a_2,a_3}\{\mu_4\} = B_0 + B_2 a_2 + B_3 a_3, \tag{17}$$

$$\mathscr{L}_{a_2,a_3}\{\mu_6\} = C_0 + C_2 a_2 + C_3 a_3. \tag{18}$$

The expressions for the coefficients A_i, B_i, and C_i as functions of α and d were derived by van Noije and Ernst [6] and by Brilliantov and Pöschel [3,18,19]. They are given in Appendix A. Obviously, $\mathscr{L}_{a_2}\{\mu_2\}$ and $\mathscr{L}_{a_2}\{\mu_4\}$ are obtained by formally setting $A_3 \to 0$ and $B_3 \to 0$ on the right-hand sides of Eqs. 16 and 17, respectively.

The exact Eq. 14 becomes an approximation when it is linearized with respect to a_2 and a_3. For $p = 2$ and $p = 3$ we get

$$\begin{aligned} 0 &= \mathscr{L}_{a_2,a_3}\left\{\mu_4 - 2\mu_2 \frac{\langle c^4\rangle}{\langle c^2\rangle}\right\} \\ &= B_0 - (d+2)A_0 + [B_2 - (d+2)(A_0 + A_2)]\, a_2 \\ &\quad + [B_3 - (d+2)A_3] a_3, \end{aligned} \tag{19}$$

$$\begin{aligned} 0 &= \mathscr{L}_{a_2,a_3}\left\{\mu_6 - 3\mu_2 \frac{\langle c^6\rangle}{\langle c^2\rangle}\right\} \\ &= C_0 - \frac{3}{4}(d+2)(d+4)A_0 + \left[C_2 - \frac{3}{4}(d+2)(d+4)\right. \\ &\quad \left. \times (3A_0 + A_2)\right] a_2 \\ &\quad + \left[C_3 - \frac{3}{4}(d+2)(d+4)(A_3 - A_0)\right] a_3. \end{aligned} \tag{20}$$

The non-systematic character of the linearization method is made evident if one proceeds in the same way, except that Eq. 14 is rewritten in the equivalent form

$$\frac{\mu_{2p}}{\langle c^{2p}\rangle} = p \frac{\mu_2}{\langle c^2\rangle}, \quad p \geq 2. \tag{21}$$

This equation shows that the *rescaled* collisional moment $\mu_{2p}/\langle c^{2p}\rangle$ is just proportional to p. Now, instead of Eqs. 19 and 20 we have

$$\begin{aligned} 0 &= \mathscr{L}_{a_2,a_3}\left\{\frac{\mu_4}{\langle c^4\rangle} - 2\frac{\mu_2}{\langle c^2\rangle}\right\} \\ &= B_0 - (d+2)A_0 + [B_2 - B_0 - (d+2)A_2] a_2 \\ &\quad + [B_3 - (d+2)A_3] a_3, \end{aligned} \tag{22}$$

$$\begin{aligned} 0 &= \mathscr{L}_{a_2,a_3}\left\{\frac{\mu_6}{\langle c^6\rangle} - 3\frac{\mu_2}{\langle c^2\rangle}\right\} \\ &= C_0 - \frac{3}{4}(d+2)(d+4)A_0 + \left[C_2 - 3C_0 - \frac{3}{4}(d+2)\right. \\ &\quad \left. \times (d+4)A_2\right] a_2 + \left[C_3 + C_0 - \frac{3}{4}(d+2)(d+4)A_3\right] a_3. \end{aligned} \tag{23}$$

Note that Eq. 22 is obtained from Eq. 19 if one formally replaces $(d+2)A_0$ by B_0 in the coefficient of a_2. Likewise, Eq. 23 is obtained from Eq. 20 by formally replacing $\frac{3}{4}(d+2)(d+4)A_0$ by C_0 in the coefficients of a_2 and a_3. Nevertheless, the approximations (19) and (20) are different from the approximations (22) and (23), respectively, so they provide different estimates of the coefficients a_2 and a_3. Henceforth we will refer to the approximations (19) and (20), which are based on Eq. 14, with the label "a". Analogously, the approximations (22) and (23), which are based on Eq. 21, will be labeled by "b". Of course, other alternative ways of

rewriting Eq. 14 are possible [13,17]. With independence of the adopted approach (say "a" or "b"), there are two basic classes of approximations: either a_3 is neglected versus a_2 in the equation for μ_4 (but not in the equation for μ_6) or both Sonine coefficients are treated on the same footing.

3.1 Class-I approximations: $a_3 \ll a_2$

Let us first assume that a_3 can be neglected versus a_2 in either Eq. 19 (approach "a") or Eq. 22 (approach "b"):

$$0 = \mathscr{L}_{a_2}\left\{\mu_4 - 2\mu_2\frac{\langle c^4\rangle}{\langle c^2\rangle}\right\} = B_0 - (d+2)A_0 + [B_2 - (d+2)(A_0+A_2)]\,a_2, \tag{24}$$

$$0 = \mathscr{L}_{a_2}\left\{\frac{\mu_4}{\langle c^4\rangle} - 2\frac{\mu_2}{\langle c^2\rangle}\right\} = B_0 - (d+2)A_0 + [B_2 - B_0 - (d+2)A_2]a_2. \tag{25}$$

These are linear equations for a_2 whose respective solutions are

$$a_2^{\mathrm{Ia}}(\alpha) = \frac{B_0 - (d+2)A_0}{(d+2)(A_2+A_0) - B_2} = \frac{16(1-\alpha)(1-2\alpha^2)}{9+24d-(41-8d)\alpha+30(1-\alpha)\alpha^2}, \tag{26}$$

$$a_2^{\mathrm{Ib}}(\alpha) = \frac{B_0 - (d+2)A_0}{(d+2)A_2 - (B_2 - B_0)} = \frac{16(1-\alpha)(1-2\alpha^2)}{25+24d-(57-8d)\alpha-2(1-\alpha)\alpha^2}, \tag{27}$$

where in the last steps use has been made of the explicit expressions of A_0, A_2, B_0, and B_2. As recalled in Sect. 2, the method labeled here as "Ia" was the one first followed by Goldshtein and Shapiro [10], the corresponding estimate, Eq. 26, being first obtained by van Noije and Ernst [6]. The alternative method "Ib", Eq. 27, was proposed in Ref. [13]. It is interesting to note that

$$a_2^{\mathrm{Ib}} = \frac{a_2^{\mathrm{Ia}}}{1+a_2^{\mathrm{Ia}}}. \tag{28}$$

Comparison with DSMC data shows that the estimate a_2^{Ib} is superior to a_2^{Ia} for $\alpha \lesssim 0.6$ [13]. Other class-I approximations for a_2 were considered by Coppex et al. [17] and are more generally described in Appendix B.

Once a_3 has been neglected in Eqs. 19 and (22), we can use Eq. 20 (approach "a") or Eq. 23 (approach "b") to express a_3 in terms of a_2. The respective results are

$$a_3^{\mathrm{Ia}}(\alpha) = G_a(\alpha, a_2^{\mathrm{Ia}}(\alpha)), \tag{29}$$

$$a_3^{\mathrm{Ib}}(\alpha) = G_b(\alpha, a_2^{\mathrm{Ib}}(\alpha)), \tag{30}$$

where

$$G_a(\alpha,a_2) \equiv \left\{C_0 - \frac{3}{4}(d+2)(d+4)A_0 + \left[C_2 - \frac{3}{4}(d+2)\times(d+4)(3A_0+A_2)\right]a_2\right\} \Big/ \left[\frac{3}{4}(d+2)(d+4)\times(A_3-A_0) - C_3\right], \tag{31}$$

$$G_b(\alpha,a_2) \equiv \left\{C_0 - \frac{3}{4}(d+2)(d+4)A_0 + \left[C_2 - 3C_0 - \frac{3}{4}(d+2)(d+4)A_2\right]a_2\right\} \Big/ \left[\frac{3}{4}(d+2)\times(d+4)A_3 - C_3 - C_0\right]. \tag{32}$$

It is also possible to construct a *hybrid* approximation "Ih" in which a_2 is obtained from Eq. 25 and a_3 is subsequently obtained from Eq. 20. In that case, $a_2^{\mathrm{Ih}} = a_2^{\mathrm{Ib}}$ while

$$a_3^{\mathrm{Ih}}(\alpha) = G_a(\alpha, a_2^{\mathrm{Ib}}(\alpha)). \tag{33}$$

The other hybrid possibility $a_3 = G_b(\alpha, a_2^{\mathrm{Ia}}(\alpha))$ turns out to be rather poor and will not be further considered here.

3.2 Class-II approximations: $a_3 \sim a_2$

If a_3 is formally treated as being of the same order as a_2, Eqs. 19 and 20 become a linear set of two coupled equations for a_2 and a_3 (approach "a"). This was the method recently considered by Brilliantov and Pöschel [18,19]. Now the problem is algebraically more involved than in the class-I approximation. The solution for a_2 is

$$a_2^{\mathrm{IIa}}(\alpha) = \frac{N_a(\alpha)}{D_a(\alpha)}, \tag{34}$$

where

$$N_a(\alpha) \equiv C_3B_0 - C_0B_3 + (d+2)(A_3C_0 - A_0C_3) + \frac{3}{4}(d+2)\times(d+4)[A_0B_3 - (A_3-A_0)B_0 - (d+2)A_0^2], \tag{35}$$

$$D_a(\alpha) \equiv C_2B_3 - C_3B_2 + (d+2)[(A_2+A_0)C_3 - A_3C_2] + \frac{3}{4}(d+2)(d+4)[(A_3-A_0)B_2 - (A_2+3A_0)B_3 + (d+2)(A_0+A_2+2A_3)A_0]. \tag{36}$$

The corresponding result for a_3 is

$$a_3^{\mathrm{IIa}}(\alpha) = G_a(\alpha, a_2^{\mathrm{IIa}}(\alpha)). \tag{37}$$

Note that, although the same functional form $G_a(\alpha, a_2)$ appears in Eqs. 29 and 37, obviously $a_3^{\mathrm{IIa}}(\alpha) \neq a_3^{\mathrm{Ia}}(\alpha)$.

The same class-II approximation can be applied to Eqs. 22 and 23 (approach "b"). The solution is now

$$a_2^{\mathrm{IIb}}(\alpha) = \frac{N_b(\alpha)}{D_b(\alpha)}, \tag{38}$$

$$a_3^{\mathrm{IIb}}(\alpha) = G_b(\alpha, a_2^{\mathrm{IIb}}(\alpha)), \tag{39}$$

where

$$N_b(\alpha) \equiv (C_0+C_3)B_0 - C_0B_3 + (d+2)[A_3C_0 - (C_0+C_3) \times A_0] + \frac{3}{4}(d+2)(d+4)(A_0B_3 - A_3B_0), \tag{40}$$

$$D_b(\alpha) \equiv (C_2-3C_0)B_3 - (C_0+C_3)(B_2-B_0) + (d+2) \times [A_2(C_0+C_3) - A_3(C_2-3C_0)] + \frac{3}{4}(d+2)(d+4)\,[A_3(B_2-B_0) - A_2B_3]\,. \tag{41}$$

The three class-I and two class-II approximations described in this Section are summarized in Table 1. As said before, a_2^{Ia} and $a_2^{\mathrm{Ib}} = a_2^{\mathrm{Ih}}$ were already proposed in Refs. [6,13], respectively, while a_2^{IIa} and a_3^{IIa} were derived in Ref. [18,19]. All the other possibilities, to the best of our knowledge, have not been considered before.

4 Comparison with computer simulations

In order to assess the reliability of the linear estimates for the Sonine coefficients a_2 and a_3 introduced in Sect. 3, it is necessary to compare them against computer simulations. To that end, we have performed new DSMC simulations for inelastic hard disks ($d = 2$). In the case of inelastic hard spheres ($d = 3$) we have used the extensive DSMC simulations presented in Ref. [18,19]. Figure 1 compares the simulation data of a_2 with the theoretical estimates a_2^{Ia}, $a_2^{\mathrm{Ib}} = a_2^{\mathrm{Ih}}$, a_2^{IIa}, and a_2^{IIb}. It is observed that the best global agreement with computer simulations is provided by the two approaches "b", i.e., the ones based on linearization of Eq. 21, in contrast to the two approaches "a", which are based on linearization of Eq. 14. Given that the class-I estimate $a_2^{\mathrm{Ib}} = a_2^{\mathrm{Ih}}$ (where a_3 is neglected) is much simpler than the class-II estimate a_2^{IIb} (where a_3 is retained), the former is preferable to the latter. In the region $0.6 \leq \alpha \leq 1$ the four approximations practically coincide among themselves and with the simulation results, thus showing that a_2^2 and a_k with $k \geq 3$ are indeed negligible in that region. On the other hand, our simulation data for hard disks ($d = 2$) show a slight improvement of the two class-II approximations with respect to the two class-I approximations, what indicates that the influence of a_2^2 is even smaller than that of a_3 for $0.6 \leq \alpha \leq 1$. The opposite behavior appears in the case of hard spheres ($d = 3$), although a certain scatter of the data in this case prevents us from confirming or refuting the behavior observed in the two-dimensional case.

Next, we consider the third Sonine coefficient a_3. The simulation data are compared with a_3^{Ia}, a_3^{Ib}, a_3^{Ih}, a_3^{IIa}, and a_3^{IIb} in Fig. 2. It is apparent that both approaches a_3^{Ib} and a_3^{IIb} have a very poor global performance, failing to account for the rapid increase of the magnitude of a_3 when $\alpha \lesssim 0.6$. However, a good semi-quantitative agreement with computer simulations is found for a_3^{Ia}, a_3^{Ih}, and a_3^{IIa}. All of this implies that the linearization of Eq. 21 with $p = 3$ is much less accurate than the linearization of Eq. 14 with $p = 3$, in contrast to the situation with $p = 2$. Interestingly enough, among the three estimates of a_3 based on the linearization of Eq. 14 with $p = 3$, the best behavior is presented by the two class-I approximations, namely a_3^{Ia} for $d = 2$ and a_3^{Ih} for $d = 3$.

Table 1 Summary of the linear approximations considered in this paper

Label	Equations	References		Behavior of a_2		Behavior of a_3	
		a_2	a_3	$0 < \alpha < 0.6$	$0.6 < \alpha < 1$	$0 < \alpha < 0.6$	$0.6 < \alpha < 1$
Ia	$\mathscr{L}_{a_2}\{\mu_4 - 2\mu_2\langle c^4\rangle/\langle c^2\rangle\} = 0$ $\mathscr{L}_{a_2,a_3}\{\mu_6 - 3\mu_2\langle c^6\rangle/\langle c^2\rangle\} = 0$	[6]	New	Fair	Good	Good	Fair
IIa	$\mathscr{L}_{a_2,a_3}\{\mu_4 - 2\mu_2\langle c^4\rangle/\langle c^2\rangle\} = 0$ $\mathscr{L}_{a_2,a_3}\{\mu_6 - 3\mu_2\langle c^6\rangle/\langle c^2\rangle\} = 0$	[18,19]	[18,19]	Fair	Good	Fair	Good
Ib	$\mathscr{L}_{a_2}\{\mu_4/\langle c^4\rangle - 2\mu_2/\langle c^2\rangle\} = 0$ $\mathscr{L}_{a_2,a_3}\{\mu_6/\langle c^6\rangle - 3\mu_2/\langle c^2\rangle\} = 0$	[13]	New	Good	Good	Poor	Poor
IIb	$\mathscr{L}_{a_2,a_3}\{\mu_4/\langle c^4\rangle - 2\mu_2/\langle c^2\rangle\} = 0$ $\mathscr{L}_{a_2,a_3}\{\mu_6/\langle c^6\rangle - 3\mu_2/\langle c^2\rangle\} = 0$	New	New	Good	Good	Poor	Good
Ih	$\mathscr{L}_{a_2}\{\mu_4/\langle c^4\rangle - 2\mu_2/\langle c^2\rangle\} = 0$ $\mathscr{L}_{a_2,a_3}\{\mu_6 - 3\mu_2\langle c^6\rangle/\langle c^2\rangle\} = 0$	[13]	New	Good	Good	Good	Fair

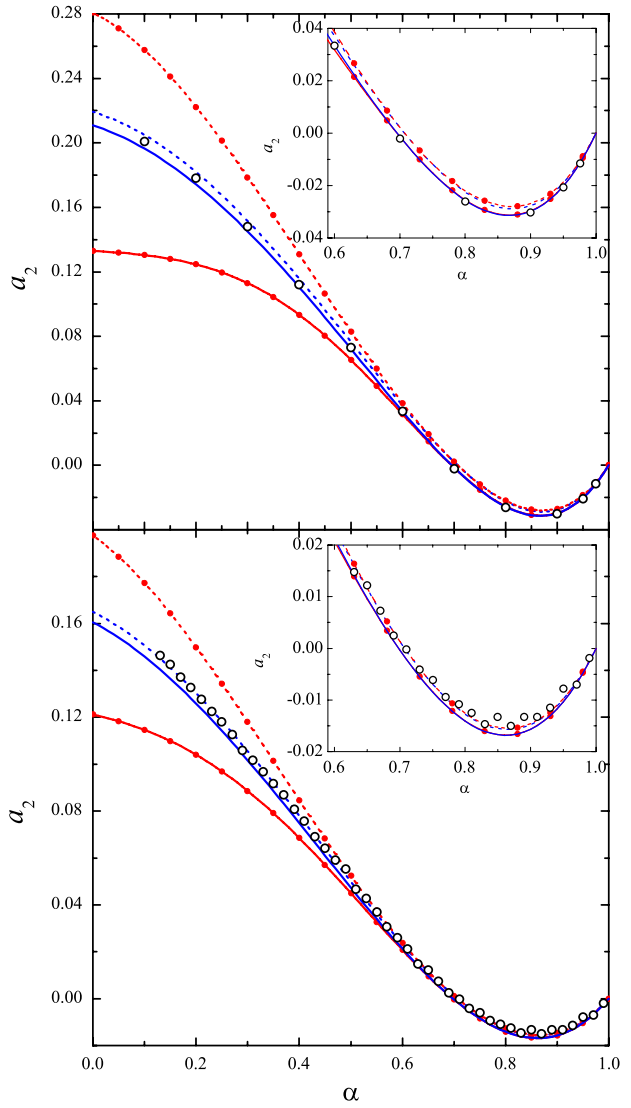

Fig. 1 (*Color online*) Plot of the second Sonine coefficient a_2 as a function of the coefficient of restitution α for $d = 2$ (*top panel*) and $d = 3$ (*bottom panel*). The *circles* represent DSMC results ($d = 2$: this work; $d = 3$: Ref. [18,19]), while the lines correspond to a_2^{Ia} (- -●- -), $a_2^{\mathrm{Ib}} = a_2^{\mathrm{Ih}}$ (- - -), a_2^{IIa} (—●—), and a_2^{IIb} (——). The insets magnify the region $0.6 \leq \alpha \leq 1$

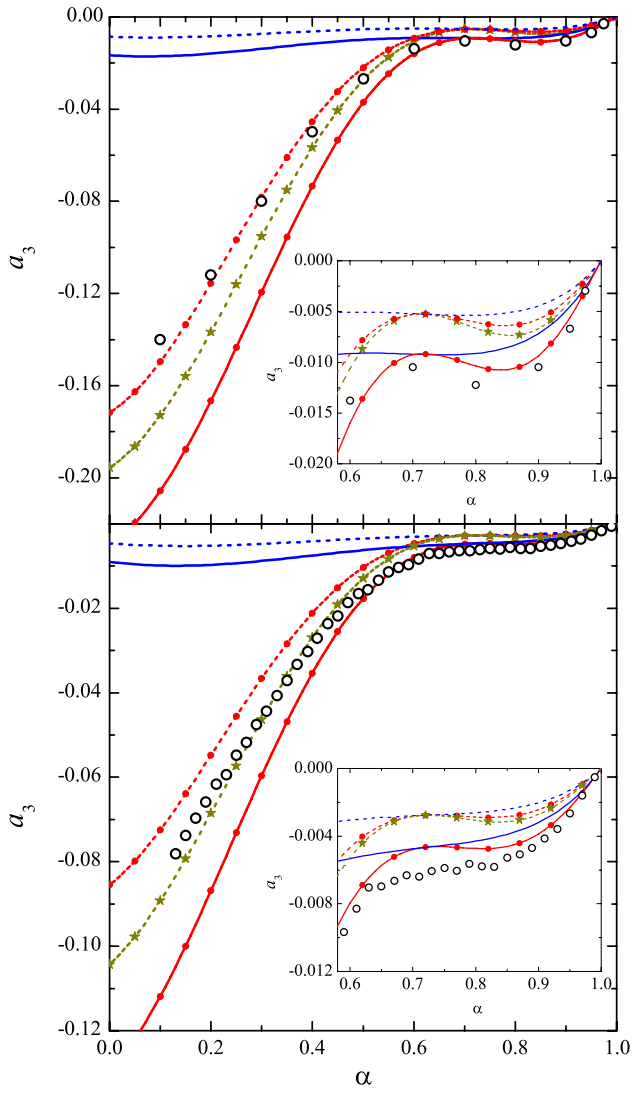

Fig. 2 (*Color online*) Plot of the third Sonine coefficient a_3 as a function of the coefficient of restitution α for $d = 2$ (*top panel*) and $d = 3$ (*bottom panel*). The circles represent DSMC results ($d = 2$: this work; $d = 3$: Ref. [18,19]), while the lines correspond to a_3^{Ia} (- -●- -), a_3^{Ib} (- - -), a_3^{Ih} (- -★- -), a_3^{IIa} (—●—), and a_3^{IIb} (——). The insets magnify the region $0.6 \leq \alpha \leq 1$

As for the region $0.6 \leq \alpha \leq 1$, the two class-II approximations are the most accurate ones. This can be understood as a consequence of the better behavior of a_2^{IIa} and a_2^{IIb} over a_2^{Ia} and a_2^{Ib} in that region, as discussed above in connection with Fig. 1.

The performance of the five linear approximations is succintly summarized in Table 1. The best global agreement with simulations is achieved by the approximation "Ih", i.e., a_2 is autonomously obtained by linearizing Eq. 21 with $p = 2$ and neglecting a_3. Next, a_3 is obtained in terms of a_2 and α from the linearization of Eq. 14 with $p = 3$. The second best combination is "IIa", where a_2 and a_3 are simultaneously derived from linearization of Eq. 14 with $p = 2$ and $p = 3$. While "Ih" is simpler than "IIa", it provides a better estimate of a_2 and a_3 for high inelasticity ($\alpha \lesssim 0.6$). This comes from a fortunate cancelation of errors and is yet another indication on the non-negligible character of nonlinear terms and higher-order Sonine coefficients in that region [18,19]. On the other hand, the best estimate of a_3 for $0.6 < \alpha < 1$ is provided by a_3^{IIa}.

Let us now define the deviations

$$\delta\mu_2 \equiv \mu_2 - \mathscr{L}_{a_2}\{\mu_2\}, \tag{42}$$

$$\delta\widetilde{\mu}_2 \equiv \mu_2(1+a_2) - \mathscr{L}_{a_2}\{\mu_2(1+a_2)\}, \tag{43}$$

Table 2 DSMC values [13] of a_2, μ_2, μ_4, $\delta\mu_2$, $\delta\widetilde{\mu}_2$, $\delta\mu_4$, and $\delta\widetilde{\mu}_4$ for $d = 3$

α	a_2	μ_2	μ_4	$\delta\mu_2$	$\delta\widetilde{\mu}_2$	$\delta\mu_4$	$\delta\widetilde{\mu}_4$
0.8	−0.0141	0.8950	4.414	−0.005	−0.005	−0.01	−0.01
0.6	0.0207	1.6101	8.213	0.000	0.000	0.03	0.02
0.4	0.0760	2.1354	11.494	0.000	0.002	0.09	0.02
0.2	0.1274	2.4625	13.881	−0.001	0.006	0.20	0.02

$$\delta\mu_4 \equiv \mu_4 - \mathscr{L}_{a_2}\{\mu_4\}, \tag{44}$$

$$\delta\widetilde{\mu}_4 \equiv \frac{\mu_4}{1+a_2} - \mathscr{L}_{a_2}\left\{\frac{\mu_4}{1+a_2}\right\}. \tag{45}$$

Consequently,

$$\mathscr{L}_{a_2}\left\{\mu_4 - 2\mu_2\frac{\langle c^4\rangle}{\langle c^2\rangle}\right\} = (d+2)\delta\widetilde{\mu}_2 - \delta\mu_4, \tag{46}$$

$$\mathscr{L}_{a_2}\left\{\frac{\mu_4}{\langle c^4\rangle} - 2\frac{\mu_2}{\langle c^2\rangle}\right\} = \frac{4}{d(d+2)}\left[(d+2)\delta\mu_2 - \delta\widetilde{\mu}_4\right]. \tag{47}$$

The fact that $a_2^{\mathrm{Ib}} = a_2^{\mathrm{Ih}}$ exhibits a better agreement with simulations than a_2^{Ia} in the high-inelasticity region obviously implies that $(d+2)\delta\mu_2 - \delta\widetilde{\mu}_4 \approx 0$ is a better approximation than $(d+2)\delta\widetilde{\mu}_2 - \delta\mu_4 \approx 0$ in that region. In principle, this does not necessarily mean that $\delta\mu_2 \approx 0$ and $\delta\widetilde{\mu}_4 \approx 0$ are better approximations than $\delta\widetilde{\mu}_2 \approx 0$ and $\delta\mu_4 \approx 0$, respectively, since a certain cancelation of terms might occur in the difference $(d+2)\delta\mu_2 - \delta\widetilde{\mu}_4$. To clarify this point, Table 2 shows a_2, μ_2, μ_4, $\delta\mu_2$, $\delta\widetilde{\mu}_2$, $\delta\mu_4$, and $\delta\widetilde{\mu}_4$ as obtained from DSMC simulations for inelastic hard spheres ($d = 3$) [13]. We can observe that one typically has $|\delta\mu_2| < |\delta\widetilde{\mu}_2|$ and $|\delta\widetilde{\mu}_4| < |\delta\mu_4|$. Moreover, $|\delta\mu_2|$ and $|\delta\widetilde{\mu}_2|$ are considerably smaller than $|\delta\mu_4|$ and $|\delta\widetilde{\mu}_4|$, thus implying that the errors made when linearizing μ_4 or $\mu_4/(1+a_2)$ are generally larger than those made when linearizing μ_2 or $\mu_2(1+a_2)$. Therefore, the property $|\delta\widetilde{\mu}_4| < |\delta\mu_4|$ is sufficient to justify that the estimate of a_2 obtained by setting $\delta\mu_2 \to 0$ and $\delta\widetilde{\mu}_4 \to 0$ in Eq. 47 is more accurate than the one obtained by setting $\delta\widetilde{\mu}_2 \to 0$ and $\delta\mu_4 \to 0$ in Eq. 46.

5 White-noise thermostat

Thus far we have assumed granular gases in the freely cooling state. The scaled quantities in this state are fully equivalent to those of granular gases kept in a steady state by a Gaussian thermostat [13], i.e., by the action of a deterministic non-conservative force proportional to the particle velocity. On the other hand, a popular way of mimicking agitated granular gases is by means of a stochastic force assumed to have the form of a Gaussian white noise [26–29].

A simple estimate of a_2 in the case of the white-noise thermostat was derived by van Noije and Ernst [6] and shown to be in excellent agreement with computer simulations [13]. However, to the best of our knowledge, an analytical expression for a_3 has not been proposed so far. The aim of this section is to fill this gap by applying linear approximations and exploiting the knowledge of the coefficients A_i, B_i, and C_i in Eqs. 16–18 [3,6,18,19]. The starting point is the moment hierarchy, which now reads [6,13]

$$\mu_{2p} = p\frac{d+2p-2}{d}\mu_2\langle c^{2p-2}\rangle, \quad p \geq 2, \tag{48}$$

or, equivalently,

$$\frac{\mu_{2p}}{\langle c^{2p-2}\rangle} = p\frac{d+2p-2}{d}\mu_2, \quad p \geq 2. \tag{49}$$

In the class-I approximation, one takes $p = 2$ and linearizes with respect to a_2, i.e.,

$$\mathscr{L}_{a_2}\{\mu_4 - (d+2)\mu_2\} = 0. \tag{50}$$

This condition is independent of whether we linearize Eq. 48 or Eq. 49, in contrast to the free cooling case. The solution of Eq. 50 is

$$a_2^{\mathrm{Ia}} = a_2^{\mathrm{Ib}} = \frac{B_0 - (d+2)A_0}{(d+2)A_2 - B_2} = \frac{16(1-\alpha)(1-2\alpha^2)}{73+56d-3(35+8d)\alpha+30(1-\alpha)\alpha^2}. \tag{51}$$

This is the result obtained in Ref. [6]. Once a_2 is known, a_3 is determined from

$$\mathscr{L}_{a_2,a_3}\left\{\mu_6 - 3\frac{d+4}{d}\mu_2\langle c^4\rangle\right\} = 0 \tag{52}$$

in the approximation "Ia" or from

$$\mathscr{L}_{a_2,a_3}\left\{\frac{\mu_6}{\langle c^4\rangle} - 3\frac{d+4}{d}\mu_2\right\} = 0 \tag{53}$$

in the approximation "Ib". The results are

$$a_3^{\mathrm{Ia}}(\alpha) = G_a(\alpha, a_2^{\mathrm{Ia}}(\alpha)), \tag{54}$$

$$a_3^{\mathrm{Ib}}(\alpha) = G_b(\alpha, a_2^{\mathrm{Ia}}(\alpha)), \tag{55}$$

where

$$G_a(\alpha,a_2)\equiv\left\{C_0-\frac{3}{4}(d+2)(d+4)A_0+\left[C_2-\frac{3}{4}(d+2)\times(d+4)(A_0+A_2)\right]a_2\right\}\Big/\left[\frac{3}{4}(d+2)(d+4)\times A_3-C_3\right], \tag{56}$$

$$G_b(\alpha,a_2)\equiv\left\{C_0-\frac{3}{4}(d+2)(d+4)A_0+\left[C_2-C_0-\frac{3}{4}(d+2)(d+4)A_2\right]a_2\right\}\Big/\left[\frac{3}{4}(d+2)\times(d+4)A_3-C_3\right]. \tag{57}$$

In the class-II approximations both a_2 and a_3 are simultaneously obtained from

$$\mathscr{L}_{a_2,a_3}\{\mu_4-(d+2)\mu_2\}=0 \tag{58}$$

and either Eq. 52 (approximation "IIa") or Eq. 53 (approximation "IIb"). The solutions are

$$a_2^{\mathrm{IIa}}(\alpha)=\frac{N_a(\alpha)}{D_a(\alpha)},\quad a_3^{\mathrm{IIa}}(\alpha)=G_a(\alpha,a_2^{\mathrm{IIa}}(\alpha)), \tag{59}$$

$$a_2^{\mathrm{IIb}}(\alpha)=\frac{N_b(\alpha)}{D_b(\alpha)},\quad a_3^{\mathrm{IIb}}(\alpha)=G_b(\alpha,a_2^{\mathrm{IIb}}(\alpha)), \tag{60}$$

where

$$N_a(\alpha)\equiv C_3B_0-C_0B_3+(d+2)(A_3C_0-A_0C_3)+\frac{3}{4}(d+2)\times(d+4)(A_0B_3-A_3B_0), \tag{61}$$

$$D_a(\alpha)\equiv C_2B_3-C_3B_2+(d+2)(A_2C_3-A_3C_2)+\frac{3}{4}(d+2)(d+4)[A_3B_2-A_2B_3+(d+2)A_0A_3-A_0B_3], \tag{62}$$

$$N_b(\alpha)=N_a(\alpha), \tag{63}$$

$$D_b(\alpha)\equiv(C_2-C_0)B_3-C_3B_2+(d+2)[A_2C_3-A_3(C_2-C_0)]+\frac{3}{4}(d+2)(d+4)(A_3B_2-A_2B_3). \tag{64}$$

Figure 3 shows the α-dependence of $a_2^{\mathrm{Ia}}=a_2^{\mathrm{Ib}}$, a_2^{IIa}, and a_2^{IIb}. The three curves are very close each other, which indicates that a_2^2 and a_k with $k\geq 3$ are indeed small enough to be neglected in $\mu_4=(d+2)\mu_2$. It is interesting to note that a_2^{IIa} and a_2^{IIb} are practically identical in the region $0.6\leq\alpha\leq 1$, where they are slightly more accurate (at least in the three-dimensional case) than $a_2^{\mathrm{Ia}}=a_2^{\mathrm{Ib}}$. On the other hand, $a_2^{\mathrm{Ia}}=a_2^{\mathrm{Ib}}$ and a_2^{IIb} are practically indistinguishable in the region of small α. The theoretical predictions a_3^{Ia}, a_3^{Ib}, a_3^{IIa}, and a_3^{IIb} are displayed in Fig. 4. Although there are no simulation data to compare with, it seems plausible to conjecture that the trends observed in Fig. 2 are repeated now:

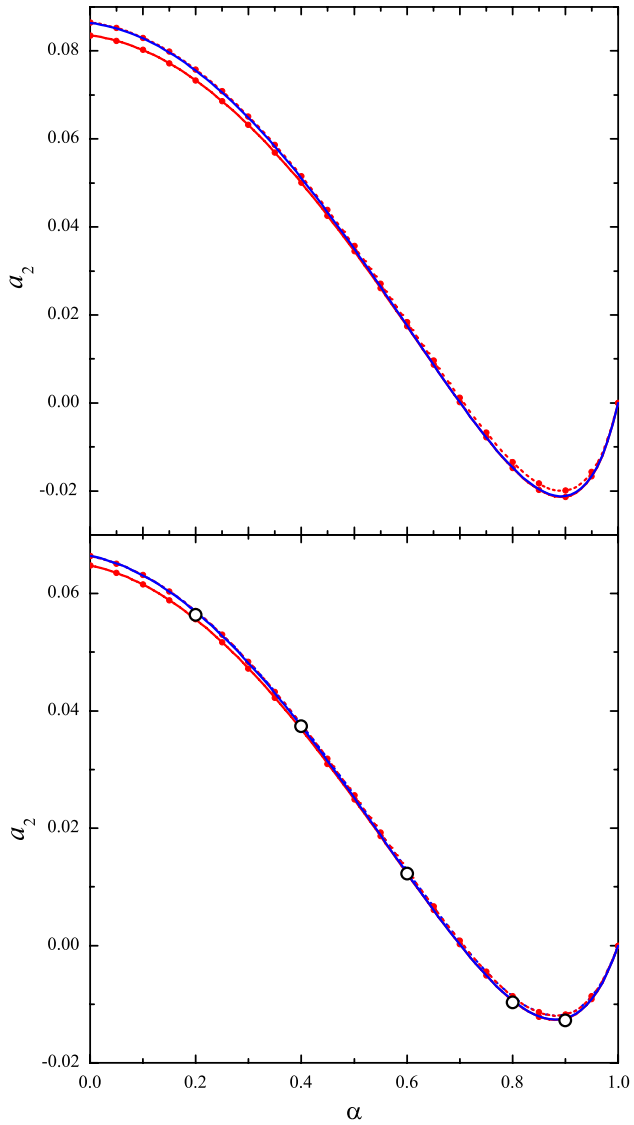

Fig. 3 (*Color online*) Plot of the second Sonine coefficient a_2 as a function of the coefficient of restitution α in the case of the white-noise thermostat for $d=2$ (*top panel*) and $d=3$ (*bottom panel*). The circles in the *bottom panel* represent DSMC results from Ref. [13], while the lines correspond to $a_2^{\mathrm{Ia}}=a_2^{\mathrm{Ib}}$ (- -●- -), a_2^{IIa} (—●—), and a_2^{IIb} (——)

the two class-II approximations are more accurate than the two class-I approximations for small dissipation, a_3^{IIa} being possibly better than a_3^{IIb}, while the two "b" approximations are rather poor at high dissipation. Note that, since $a_2^{\mathrm{Ia}}=a_2^{\mathrm{Ib}}$ in the case of the white-noise thermostat, the hybrid approximation "Ih" coincides with "Ia", i.e., $a_3^{\mathrm{Ih}}=a_3^{\mathrm{Ia}}$. A feature that becomes apparent when comparing Figs. 1 and 2 with Figs. 3 and 4, respectively, is that the magnitudes of a_2 and a_3 in the white-noise case are about twice and ten times, respectively, smaller than those in the freely cooling state. This is closely related to the fact that the overpopulation of the high-energy tail is much smaller in the former case than in the latter. More specifically, instead of Eq. 10, now we have [6]

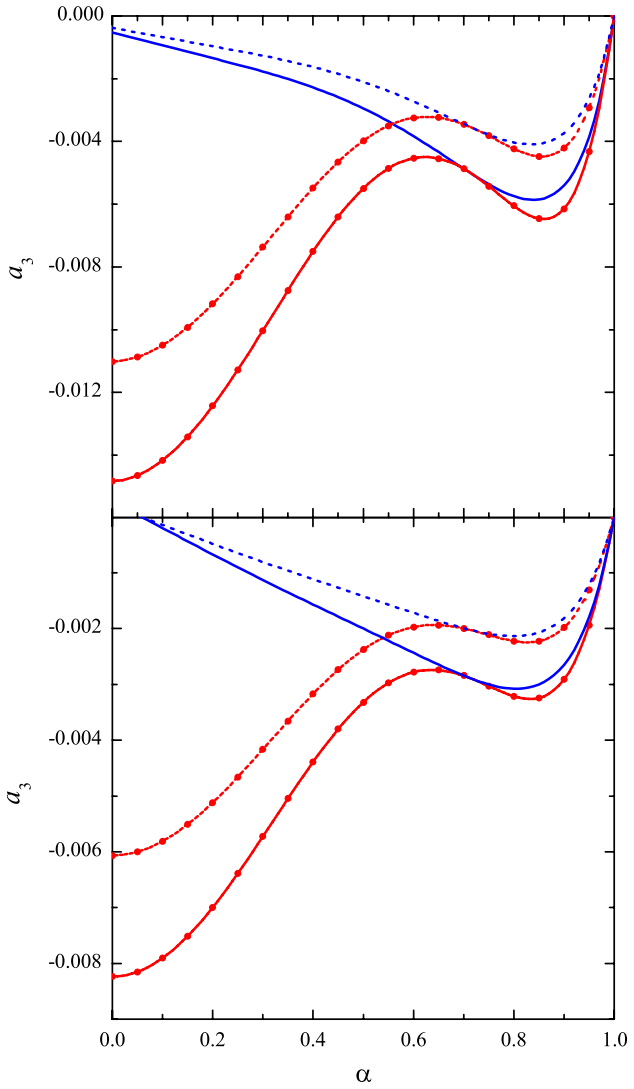

Fig. 4 (*Color online*) Plot of the third Sonine coefficient a_3 as a function of the coefficient of restitution α in the case of the white-noise thermostat for $d = 2$ (*top panel*) and $d = 3$ (*bottom panel*). The lines correspond to a_3^{Ia} (- -•- -), a_3^{Ib} (- - -), a_3^{IIa} (—•—), and a_3^{IIb} (——)

$$F(\mathbf{c}) \sim e^{-\frac{2}{3}\sqrt{2\xi c^3}}, \tag{65}$$

where ξ is the same quantity as in Eq. 10.

6 Conclusions

The second and third coefficients in the Sonine polynomial expansion of the (scaled) velocity distribution function $F(\mathbf{c})$ of a granular gas characterize the deviation of $F(\mathbf{c})$ from the Maxwellian and are important, for instance, in the precise determination of transport coefficients. While for practical purposes an interval $0.8 \lesssim \alpha < 1$ for the coefficient of normal restitution is sufficient, it becomes necessary from a more fundamental viewpoint to consider the whole range $0 < \alpha < 1$.

The Sonine coefficients $a_2(\alpha)$ and $a_3(\alpha)$ can be measured in computer simulations (e.g., DSMC), so one could in principle make a least-square fit to certain functional forms. However, this would not be satisfactory from a fundamental point of view and would not provide any insight into the intricacies of $F(\mathbf{c})$ and its Sonine expansion. It is then much more challenging to devise theoretical approximations that can be subsequently assessed by comparison with simulation results.

In this paper we have been mainly concerned with a family of linear approximations to estimate $a_2(\alpha)$ and $a_3(\alpha)$ in the freely cooling state. We have found that a good compromise between accuracy and simplicity is represented by the hybrid approximation here denoted as "Ih", in which the second and third Sonine coefficients are given by Eqs. 27 and 33, respectively. For the benefit of the reader here we quote the final and complete expressions:

$$a_2(\alpha) = \frac{16(1-\alpha)(1-2\alpha^2)}{25+24d-(57-8d)\alpha-2(1-\alpha)\alpha^2}, \tag{66}$$

$$a_3(\alpha) = -\frac{16a_2(\alpha)}{1-2\alpha^2}\frac{P_{\text{HCS}}(\alpha)}{Q_{\text{HCS}}(\alpha)}, \tag{67}$$

where

$$\begin{aligned} P_{\text{HCS}}(\alpha) = {} & 167+50d-(191+26d)\alpha-2(307+100d)\alpha^2 \\ & +2(339+68d)\alpha^3+32(16+7d)\alpha^4 \\ & -32(18+5d)\alpha^5+144(1-\alpha)\alpha^6, \end{aligned} \tag{68}$$

$$\begin{aligned} Q_{\text{HCS}}(\alpha) = {} & 521+1396d+368d^2-(1481+820d \\ & -16d^2)\alpha+4(583+262d)\alpha^2 \\ & -20(155+14d)\alpha^3+280(1-\alpha)\alpha^4 \end{aligned} \tag{69}$$

However, if more precise values in the domain $0.6 \leq \alpha < 1$ are really needed, it might be preferable to consider the more complicated approximation "IIa" given by Eqs. 34 and 37 [18,19].

On the other hand, It is known that in the high-inelasticity region $\alpha \lesssim 0.6$ (i.e., once a_2 becomes positive) the higher-order Sonine coefficients are no longer negligible [9,15,18,19], so that the linear approximations based on the neglect of nonlinear terms and of a_k with $k \geq 3$ or $k \geq 4$ are not a priori reliable. This is made evident by the lack of self-consistency of different linear approximations used to estimate a_2 from the first non-trivial equation of the moment hierarchy, as shown in Fig. 1. What is indeed surprising is that the simple linear approximation (66) provides such an excellent estimate both for $d = 2$ and $d = 3$. This means that, even though a_2^2, a_3, a_4, …are not negligible at all if $\alpha \lesssim 0.6$, somehow they practically cancel out in the combination $\mu_4/\langle c^4\rangle - 2\mu_2/\langle c^2\rangle$, while still playing a significant role in the combination $\mu_4 - 2\mu_2\langle c^4\rangle/\langle c^2\rangle$. This is clearly

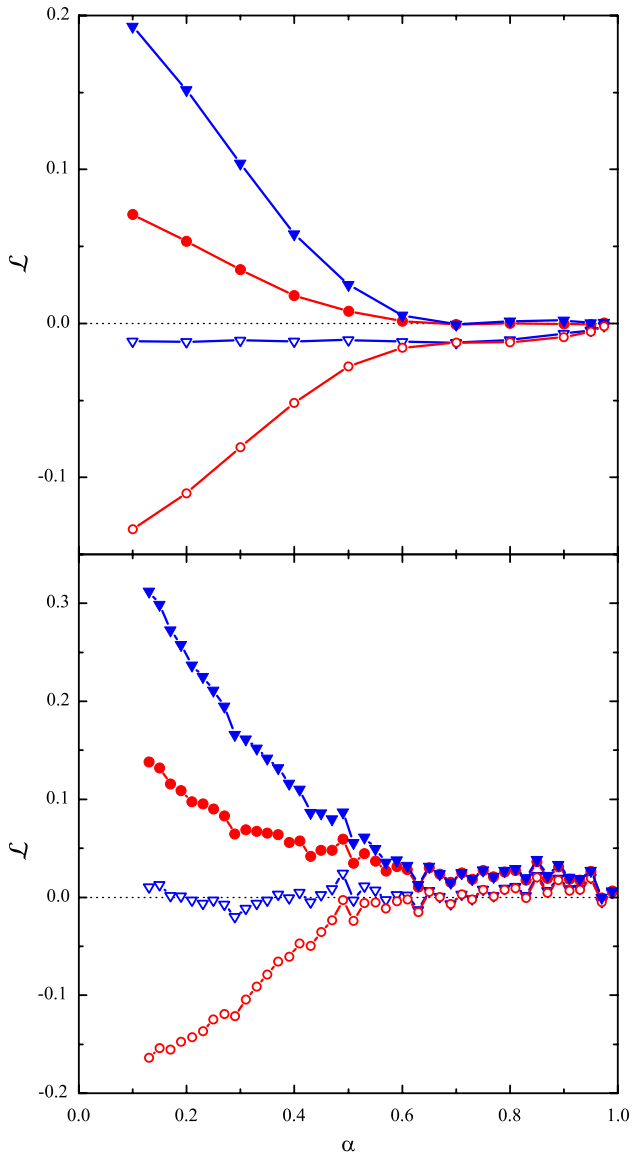

Fig. 5 (*Color online*) Plot of $\mathscr{L}_{a_2}\{\mu_4-(d+2)\mu_2(1+a_2)\}$ (○), $\mathscr{L}_{a_2,a_3}\{\mu_4-(d+2)\mu_2(1+a_2)\}$ (●), $\mathscr{L}_{a_2}\{\mu_4/(1+a_2)-(d+2)\mu_2\}$ (▽), and $\mathscr{L}_{a_2,a_3}\{\mu_4/(1+a_2)-(d+2)\mu_2\}$ (▼) for $d=2$ (*top panel*) and $d=3$ (*bottom panel*). The *symbols* are obtained from DSMC results of a_2 and a_3 ($d=2$: this work; $d=3$: Ref. [18,19]). The lines are guides to the eye

seen in Fig. 5, where we plot $\mathscr{L}_{a_2}\{\mu_4-(d+2)\mu_2(1+a_2)\}$, $\mathscr{L}_{a_2,a_3}\{\mu_4-(d+2)\mu_2(1+a_2)\}$, $\mathscr{L}_{a_2}\{\mu_4/(1+a_2)-(d+2)\mu_2\}$, and $\mathscr{L}_{a_2,a_3}\{\mu_4/(1+a_2)-(d+2)\mu_2\}$ by using the simulation data of a_2 and a_3. While the magnitude of the other three quantities rapidly increases with increasing inelasticity if $\alpha\lesssim 0.6$, that of $\mathscr{L}_{a_2}\{\mu_4/(1+a_2)-(d+2)\mu_2\}$ remains small and practically constant. This property might be useful to contribute to a better understanding of the full velocity distribution function $F(\mathbf{c})$.

Although this paper has focused on the HCS, the analysis has been straightforwardly extended in Sect. 5 to a granular gas heated by a white-noise thermostat. In that case, the optimal combination of estimates is provided by Eqs. 51 and 54. More specifically,

$$a_2=\frac{16(1-\alpha)(1-2\alpha^2)}{73+56d-3(35+8d)\alpha+30(1-\alpha)\alpha^2}, \tag{70}$$

$$a_3(\alpha)=-\frac{16a_2(\alpha)}{1-2\alpha^2}\frac{P_{\rm WN}(\alpha)}{Q_{\rm WN}(\alpha)}, \tag{71}$$

where

$$\begin{aligned}P_{\rm WN}(\alpha)&=67+10d-7(13-2d)\alpha-2(119+20d)\alpha^2\\&\quad+2(151-12d)\alpha^3+32(8+3d)\alpha^4\\&\quad-32(10+d)\alpha^5+80(1-\alpha)\alpha^6,\end{aligned} \tag{72}$$

$$\begin{aligned}Q_{\rm WN}(\alpha)&=2569+2932d+624d^2-(3529+2356d\\&\quad+240d^2)\alpha+4(583+262d)\alpha^2\\&\quad-20(155+14d)\alpha^3+280(1-\alpha)\alpha^4.\end{aligned} \tag{73}$$

It would be interesting to test the accuracy of Eq. 71 against computer simulations.

Appendix A: Expressions for A_i, B_i, and C_i

The explicit expressions of the coefficients A_i, B_i, and C_i as functions of d and α are [3,6,18,19]

$$A_0=K(1-\alpha^2),\quad A_2=\frac{3K}{16}(1-\alpha^2),\quad A_3=\frac{K}{64}(1-\alpha^2), \tag{74}$$

$$B_0=K(1-\alpha^2)\left(d+\frac{3}{2}+\alpha^2\right), \tag{75}$$

$$B_2=K(1+\alpha)\left[\frac{3}{32}(1-\alpha)(10d+39+10\alpha^2)+(d-1)\right], \tag{76}$$

$$\begin{aligned}B_3&=-\frac{K}{128}(1+\alpha)\\&\quad\times\left[(1-\alpha)(97+10\alpha^2)+2(d-1)(21-5\alpha)\right],\end{aligned} \tag{77}$$

$$C_0=\frac{3K}{4}(1-\alpha^2)\left[(d+\alpha^2)(5+2\alpha^2)+d^2+\frac{19}{4}\right], \tag{78}$$

$$\begin{aligned}C_2&=\frac{3K}{256}(1-\alpha^2)\\&\quad\times\left[1289+4(d+\alpha^2)(311+70\alpha^2)+172d^2\right]+\frac{3}{4}\beta,\end{aligned} \tag{79}$$

$$\begin{aligned}C_3&=-\frac{3K}{1024}(1-\alpha^2)\\&\quad\times\left[2537+4(d+\alpha^2)(583+70\alpha^2)+236d^2\right]-\frac{9}{16}\beta,\end{aligned} \tag{80}$$

where

$$K \equiv \frac{\pi^{(d-1)/2}}{\sqrt{2}\Gamma(d/2)},$$
$$\beta \equiv K(1+\alpha)\left[(d-\alpha)(3+4\alpha^2)+2(d^2-\alpha)\right]. \quad (81)$$

Appendix B: Other class-I linear approximations for a_2

As a generalization of Eqs. 24 and 25, let us consider the family of approximations

$$\mathscr{L}_{a_2}\left\{\frac{\mu_4^{1-z}}{\langle c^4\rangle^x \mu_2^y}-2\frac{\mu_2^{1-y}\langle c^4\rangle^{1-x}}{\langle c^2\rangle \mu_4^z}\right\}=0 \quad (82)$$

and let us denote by $a_2^{(x,y,z)}$ the associated solution. In particular, $a_2^{(0,0,0)} \equiv a_2^{\mathrm{Ia}}$ and $a_2^{(1,0,0)} \equiv a_2^{\mathrm{Ib}}$. The eight possibilities considered by Coppex et al. [17] correspond to $x = 0, 1$, $y = 0, 1$, and $z = 0, 1$. It is easy to check that the solution to Eq. 82 is

$$a_2^{(x,y,z)} = \frac{a_2^{\mathrm{Ia}}}{1+h_{xyz}a_2^{\mathrm{Ia}}}, \quad (83)$$

where

$$h_{xyz} \equiv x + y\frac{A_2}{A_0} + z\frac{B_2}{B_0}. \quad (84)$$

Equation 83 is a generalization of Eq. 28.

Of course, other alternative possibilities exist. For instance, one can generalize Eq. 82 to

$$\mathscr{L}_{a_2}\left\{\Phi\left(\frac{\mu_4^{1-z}}{\langle c^4\rangle^x \mu_2^y}\right)-\Phi\left(2\frac{\mu_2^{1-y}\langle c^4\rangle^{1-x}}{\langle c^2\rangle \mu_4^z}\right)\right\}=0, \quad (85)$$

where $\Phi(X)$ is an arbitrary function. The corresponding approximation for a_2 will depend on the choice of $\Phi(X)$, apart from the values of x, y, z.

Acknowledgments The authors are grateful to N. Brilliantov and T. Pöschel for providing the simulation data of Ref. [18,19]. This research has been supported by the Ministerio de Educación y Ciencia (Spain) through grants Nos. FIS2007-60977 (A.S.) and DPI2007-63559 (J.M.M.), partially financed by FEDER funds.

References

1. Campbell, C.S.: Rapid granular flows. Annu. Rev. Fluid Mech. **22**, 57 (1990)
2. Goldhirsch, I.: Rapid granular flows. Annu. Rev. Fluid Mech. **35**, 267 (2003)
3. Brilliantov, N., Pöschel, T.: Kinetic Theory of Granular Gases. Oxford University Press, Oxford (2004)
4. Brey, J.J., Dufty, J.W., Santos, A.: Dissipative dynamics for hard spheres. J. Stat. Phys. **87**, 1051 (1997)
5. Haff, P.K.: Grain flow as a fluid-mechanical phenomenon. J. Fluid Mech. **134**, 401 (1983)
6. van Noije, T.P.C., Ernst, M.H.: Velocity distributions in homogeneous granular fluids: the free and the heated case. Granul. Matter **1**, 57 (1998)
7. Esipov, S.E., Pöschel, T.: The granular phase diagram. J. Stat. Phys. **86**, 1385 (1997)
8. Abramowitz, M., Stegun, I.A. (eds.) Handbook of Mathematical Functions, Ch. 22. Dover, New York (1972)
9. Noskowicz, S.H., Bar-Lev, O., Serero, D., Goldhirsch, I.: Computer-aided kinetic theory and granular gases. Europhys. Lett. **79**, 60001 (2007)
10. Goldshtein, A., Shapiro, M.: Mechanics of collisional motion of granular materials. Part 1. General hydrodynamic equations. J. Fluid Mech. **282**, 75 (1995)
11. Brey, J.J., Ruiz-Montero, M.J., Cubero, D.: Homogeneous cooling state of a low-density granular flow. Phys. Rev. E **54**, 3664 (1996)
12. Garzó, V., Dufty, J.W.: Homogeneous cooling state for a granular mixture. Phys. Rev. E **60**, 5706 (1999)
13. Montanero, J.M., Santos, A.: Computer simulation of uniformly heated granular fluids. Granul. Matter **2**, 53 (2000)
14. Brilliantov, N., Pöschel, T.: Deviation from Maxwell distribution in granular gases with constant restitution coefficient. Phys. Rev. E **61**, 2809 (2000)
15. Huthmann, M., Orza, J.A.G., Brito, R.: Dynamics of deviations from the Gaussian state in a freely cooling homogeneous system of smooth inelastic particles. Granul. Matter **2**, 189 (2000)
16. Montanero, J.M., Garzó, V.: Monte Carlo simulation of the homogeneous cooling state for a granular mixture. Granul. Matter **4**, 17 (2002)
17. Coppex, F., Droz, M., Piasecki, J., Trizac, E.: On the first Sonine correction for granular gases. Physica A **329**, 114 (2003)
18. Brilliantov, N., Pöschel, T.: Breakdown of the Sonine expansion for the velocity distribution of granular gases. Europhys. Lett. **74**, 424 (2006)
19. Brilliantov, N., Pöschel, T.: Erratum: breakdown of the Sonine expansion for the velocity distribution of granular gases. Europhys. Lett. **75**, 188 (2006)
20. Ahmad, S.R., Puri, S.: Velocity distributions in a freely evolving granular gas. Europhys. Lett. **75**, 56 (2006)
21. Ahmad, S.R., Puri, S.: Velocity distributions and aging in a cooling granular gas. Phys. Rev. E **75**, 031302 (2007)
22. Brey, J.J., Dufty, J.W., Kim, C.S., Santos, A.: Hydrodynamics for granular flow at low density. Phys. Rev. E **58**, 4638 (1998)
23. Garzó, V., Santos, A., Montanero, J.M.: Modified Sonine approximation for the Navier-Stokes transport coefficients of a granular gas. Physica A **376**, 94 (2007)
24. Bird, G.: Molecular Gas Dynamics and the Direct Simulation of Gas Flows. Clarendon, Oxford (1994)
25. Alexander, F.J., Garcia, A.L.: The direct simulation Monte Carlo method. Comp. Phys. **11**, 588 (1997)
26. Williams, D.R.M., MacKintosh, F.C.: Driven granular media in one dimension: correlations and equation of state. Phys. Rev. E **54**, R9 (1996)
27. Williams, D.R.M.: Driven granular media and dissipative gases: correlations and liquid-gas phase transitions. Physica A **233**, 718 (1996)
28. Swift, M.R., Boamfă, M., Cornell, S.J., Maritan, A.: Scale invariant correlations in a driven dissipative gas. Phys. Rev. Lett. **80**, 4410 (1998)
29. Santos, A., Ernst, M.H.: Exact steady-state solution of the Boltzmann equation: a driven one-dimensional inelastic Maxwell gas. Phys. Rev. E **68**, 011305 (2003)